JOURNAL OF
biomaterials
applications

Hard Tissues and Materials

Journal of Biomaterials Applications
0(0) 1–12

DOI: 10.1177/0885328218812490
journals.sagepub.com/home/jba
SAGE

Structural and bone marrow stem cell biocompatibility studies of hydrogel synthesized via chemo-enzymatic route

Ahmad Safwan Ahmad Latfi[1], Sumit Pramanik[2], Chi Tat Poon[1], Ahmad Mohammed Gumel[3], Khin Wee Lai[1], Mohamad Suffian Mohamad Annuar[3] and Belinda Pingguan-Murphy[1]

Abstract

Natural biopolymers have many attractive medical applications; however, complications due to fibrosis caused a reduction in diffusion and dispersal of nutrients and waste products. Consequently, severe immunocompatibility problems and poor mechanical and degradation properties in synthetic polymers ensue. Hence, the present study investigates a novel hydrogel material synthesized from caprolactone, ethylene glycol, ethylenediamine, polyethylene glycol, ammonium persulfate, and tetramethylethylenediamine via chemo-enzymatic route. Spectroscopic analyses indicated the formation of polyurea and polyhydroxyurethane as the primary building block of the hydrogel starting material. Biocompatibility studies showed positive observation in biosafety test using direct contact cytotoxicity assay in addition to active cellular growth on the hydrogel scaffold based on fluorescence observation. The synthesized hydrogel also exhibited (self) fluorescence properties under specific wavelength excitation. Hence, synthesized hydrogel could be a potential candidate for medical imaging as well as tissue engineering applications as a tissue expander, coating material, biosensor, and drug delivery system.

Keywords

Polyurea, polyhydroxyurethane, neocell, cytotoxicity, fluorescence, resazurin

Introduction

A wide range of polymeric biomaterials have been used in the biomedical field. They are mainly utilized as scaffolds and implants in roles including repair, replacement, or diagnostic applications.[1–3] Hydrogel biomaterials have found widespread use in dental, skin, drug distribution, and various surgical applications.[4] The large molecular mass of the polymer contributes to the distinctive and, often advantageous, physical properties relative to the small molecule compounds. The supramolecular architecture of polymers can be designed to facilitate semicrystalline structures rather than crystalline structures, with concomitant modulation of its durability and viscoelasticity characteristics. It is relatively easy to fabricate a wide variety of compositions, properties, and forms (i.e. solids, fibers, fabrics, films, and gels) from polymers to obtain complex designs and structures. Being organic in nature, biopolymers offer many advantages over metallic and ceramic biomaterials. Furthermore, the market value of medical polymers is estimated at more than a billion dollars with an annual increase of 10–20%.[5] Hydrogels as a form of colloidal gel

[1]Department of Biomedical Engineering, Faculty of Engineering, University of Malaya, Kuala Lumpur, Malaysia
[2]Department of Mechanical Engineering, SRM Institute of Science and Technology, Chennai, India
[3]Institute of Biological Sciences, Faculty of Science, University of Malaya, Kuala Lumpur, Malaysia

Corresponding authors:
Sumit Pramanik, Department of Mechanical Engineering, SRM Institute of Science and Technology, Kattankulathur, Kancheepuram District, Chennai 603203, Tamil Nadu, India.
Email: sumitpramanik.s@ktr.srmuniv.ac.in / prsumit@gmail.com
Belinda Pingguan-Murphy, Department of Biomedical Engineering, Faculty of Engineering, University of Malaya, Kuala Lumpur 50603, Malaysia.
Email: bpingguan@um.edu.my

are normally formed from hydrophilic natural or synthetic polymer networks. The diffusion or dispersion medium is water. They are extremely absorbent and porous and sometimes can comprise over 90% water. Due to the significant water content, they are very similar to natural tissue in terms of degree of flexibility and suppleness, thus opening up a number of potential applications in biomedical fields through their resemblance to living tissues. It has been estimated that the total cost of hydrogels that have significant impact to the United States economy alone is approximately $400 billion per year.[6] The hydrogels have been utilized for making contact lenses, drug delivery and distribution systems, as contrast agents, hygiene goods, scaffolding, tissue engineering components, wound dressings, and bandages.

Tissue and organ transplantations are widely accepted and acknowledged forms of therapy and rehabilitation. However, shortages and unavailability of donors cause this type of therapy to be restricted dramatically. Hydrogels have found application in tissue engineering. They are used as delivery and distribution vehicles for bioactive substances and as space filling agents for three-dimensional (3D) structures, which arrange cells and present stimuli to promote the development and growth of obligatory tissues.[7] They could also act as biological and organic glue for bulking and to avoid adhesion. Drugs can be distributed and supplied in a variety of applications from hydrogel scaffolds. Such scaffolds have also been used to restore and resettle transplanted cells for producing large amounts of tissue, including cartilage, bone, and smooth muscle.[8] Their unique properties, including significant water content, softness, smoothness, flexibility, suppleness, and biocompatibility, make them very useful in different biomedical applications. In order to produce hydrogels, cross-linking between hydrophilic polymers has to be done by physical or chemical means, resulting in 3D network structure that mimics the microenvironment of cells.[9] Wells coated with hydrogels are also used for cell culture.[10] Specific molecules with "respond-and-react" characteristics e.g. antigen/antibody attached on the hydrogels allow for biosensing ability and modulated drug delivery systems.[11]

However, conventional hydrogels suffer from several problems e.g. fibrosis decreasing diffusion and dispersal of nutrients and waste products to/from the living cells. They also create complications such as immunocompatibility issues in conventional synthetic hydrogels. In addition, poor mechanical properties e.g. tensile strength, rapid, or inconsistent degradation curtails their extensive use.[12] Further, the attached cells risk being damaged from the cytotoxic effects of macrophage-generated nitric oxide and consequent damage of bone, dermis, intestinal, and duodenal submucosa.

The present study aims to develop a flexible biocompatible hydrogel obtained from ε-caprolactone, ethylene glycol, and ethylenediamine from lipase-mediated synthesis. Characterization of the fabricated hydrogels includes structural authentication, thermomechanical, and biocompatible tests for medical and tissue engineering applications. The biocompatibility was assessed from cytotoxicity evaluation based on direct contact of the hydrogel as a scaffold for cell attachment and growth.

Materials and methods

Lipase-mediated synthesis of hydrogel macromer

Immobilized lipase B (Novozym® 435) (which was originated from *Candida antarctica* and had already been immobilized on microporous acrylic resin) purchased from Sigma-Aldrich and ε-caprolactone (Sigma-Aldrich) were mixed together at 100:3 ratio (w/v) in reaction vials. The reaction mixture was incubated at 200 r/min at 50°C for 24 h in a shaker incubator (Labtech, Daihan Labtech Co. Ltd, Korea). Thereafter, ethylene glycol and ethylene diamine (3:1 v/v ratio) were added to the viscous reaction mixture, and incubation was continued for another 24 h.

Subsequently, the macromer was extracted by diluting the viscous reaction mixture with 5 ml dichloromethane (DCM) (∼2× initial caprolactone volume), followed by the addition of 10 ml acetone (∼2× DCM volume). Then, the lipase beads were filtered out from the mixture. A gel-like material was precipitated out from the filtrate solution at room temperature (25°C ± 1°C).

In the synthesis of the lipase-mediated biomaterial, a condensation polymerization occurred. Lipase was used as an enzyme to catalyze the ring-opening polymerization.[13,14] Caprolactone undergoes ring-opening polymerization by the enzyme lipase (see Scheme 1(a)). Ethylene glycol and ethylenediamine on the other hand undergo condensation polymerization. The –OH group from the ethylene glycol and the hydrogen from the $–NH_2$ group of the ethylenediamine reacted together by forming water (H_2O). The H_2O influenced the functional groups (–OH from ethylene glycol and $–NH_2$ from ethylenediamine) to react with caprolactone in order to produce polyhydroxyurethane (PHU) and polyurea (PU). Therefore, two different probable polymerization reactions were occurred (see Scheme 1(b) and (c)). All the potential reactions are summarized in Scheme 1.

Synthesis of hydrogels

The hydrogels were synthesized using a polymerization method described by Gumel et al.[15] with a slight modification. It involved a free radical polymerization of

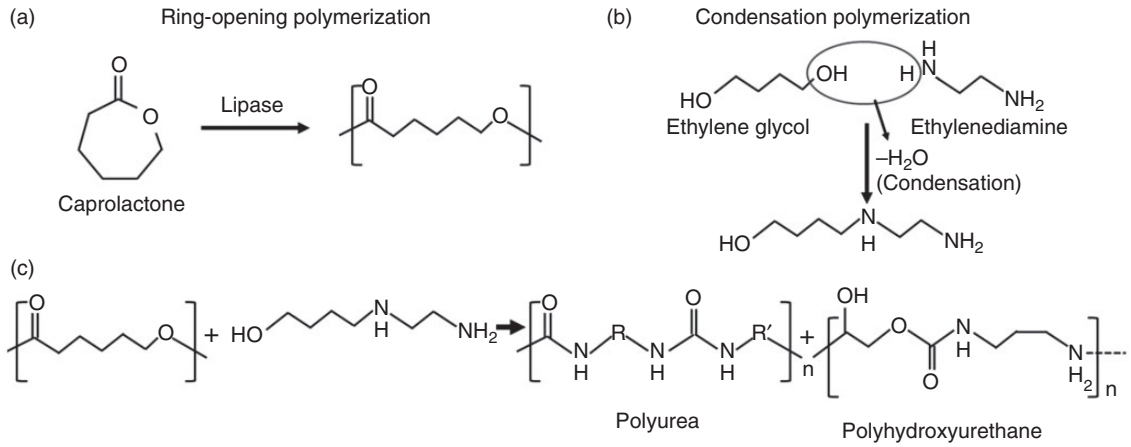

Scheme 1. (a) Ring-opening polymerization of the caprolactone catalyzed by the enzyme lipase. (b) Condensation polymerization of ethylene glycol and ethylenediamine, producing water. (c) The mixture of both products from (a) and (b) producing polyurea and polyhydroxyurethane.

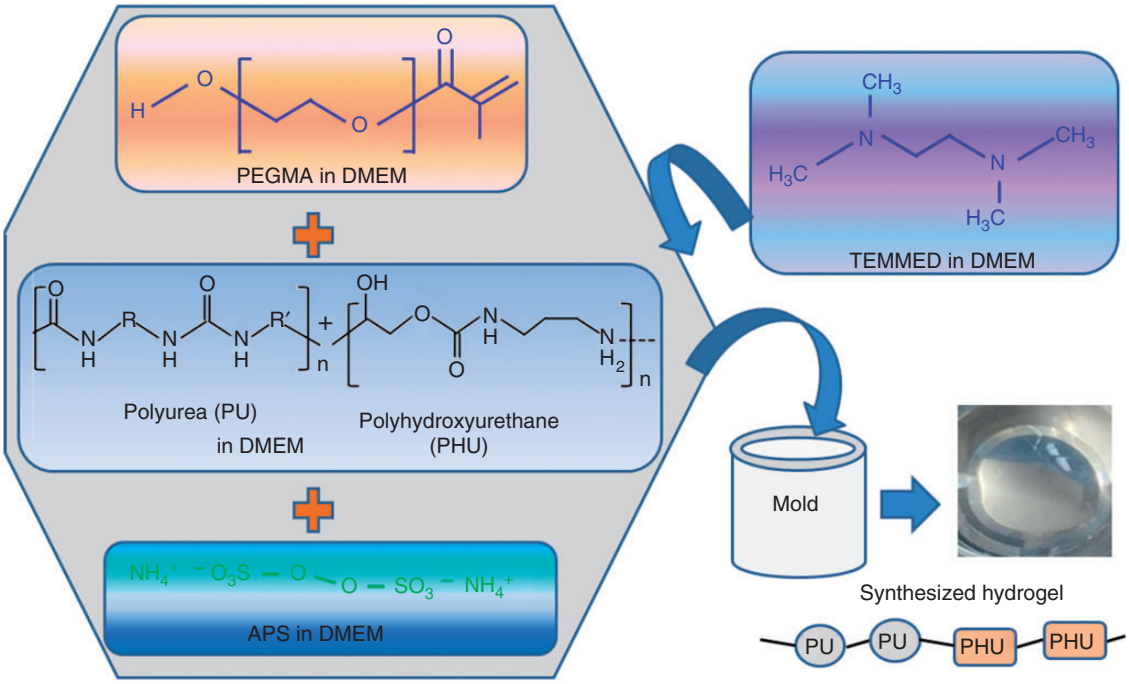

Scheme 2. A schematic diagram of hydrogel preparation. (Color image is available only for soft copy in online and not for printed copy).

four main reactants viz. gel-like synthesized material as described in the previous section, polyethylene glycol methacrylate (PEGMA), ammonium persulfate (APS), and tetramethyldiamine (TEMED). Each material was individually subjected to a high power ultraviolet (UV) radiation treatment for an hour using UV lamp equipped in laminar flow hood (Safemate 1.2, Bioair) prior to their use in the polymerization reaction. The first solution consisting of gel-like material was produced by dissolving it completely in DMEM at 1:2 (w/v) ratio followed by vortex-mixing. The second solution consisted of PEGMA in DMEM at 1:2 (w/v) ratio followed by vortex-mixing for 1 s. The PEGMA solution was used to form extensive network. The third solution of APS in DMEM at 1:10 (w/v) ratio was prepared followed by vortex-mixing. Each of the three solutions was mixed according to weight ratio of 25:25:1 in a centrifuge tube. Then, TEMED solution (at 1:2 v/v ratio TEMED:DMEM) was added to the resulting mixture at 1:6 (v/v) followed by vortex-

mixing. Thereafter, the whole mixture was poured into a proper mold. A schematic diagram of hydrogel preparation is shown in Scheme 2. For thermal and thermomechanical analyses, a plastic straw of 8 mm diameter was used as a mold. For biological assays, the wells of 96-well plate were used as mold. Approximately 15 ml solution was poured in each straw and 100 µl was poured in each well of the 96-well plate. The pouring step was rapidly done as the mixture hardens within a short period following the addition of TEMED solution. For the straw mold, early solidification of the mixture occurred within the first five minutes inside the straw tube with both ends sealed. Then, the soft solid was left at room temperature for another 15–20 min to obtain the hydrogel structure. Subsequently, the hydrogel was gently pushed out of the straw mold into a petri dish by squeezing the tube. Then, it was cut into several pieces of approximately 10 mm length. The hydrogel from the 96-well mold was also taken out gently. All hydrogels were soaked in a sterile distilled water before being subjected to further characterizations.

For biological assays, sterilized distilled water was freshly changed every day to remove unwanted leaching carry-over compounds. The discarded distilled water was subjected to pH measurement. The soaking process was repeated until the pH of the discarded solution indicated neutrality. Then, soaking was continued for another one week in an incubator with 5% CO_2 atmosphere at 37°C to get rid of residual unwanted compounds.

Hydrogel characterizations

Fourier transform infrared spectroscopy. The functional groups of the hydrogel material were determined by Fourier transform infrared (FTIR) spectroscopy (400, Perkin Elmer, Waltham, UK). For the analysis, samples were placed on monolithic diamond attenuated total reflectance probe and clamped against the diamond crystal plate using a force adapter. Thereafter, the samples were scanned over a range of 4000–400 cm^{-1} at 25°C.

Nuclear magnetic resonance spectroscopy. The chemical structure of the hydrogel material was authenticated using ^{1}H and ^{13}C nuclear magnetic resonance (NMR) spectroscopy at 600 MHz (AVANCE III 600 MHz, Bruker, Massachusetts, USA). Twenty milligrams of the material was prepared in a glass vial and completely dissolved in 1 ml deuterated dimethyl sulfoxide (DMSO-d_6) solvent for overnight (12 h). The glass vial was then covered with aluminum foil and placed on a shaker at 100 r/min for 1 h. Then, the samples were transferred into a 5-mm diameter NMR tube prior to analysis.

Thermogravimetric analysis. Thermal stability of the synthesized dry and wet hydrogels was analyzed by thermogravimetric analysis (TGA) (Q500, TA Instrument, New Castle, USA). It was performed in nitrogen atmosphere, with a heating rate of 10°C min^{-1}, 40–600°C as described by Manna et al.[16] The surface water from both the hydrogel samples was completely removed by soaking with dry tissue paper before the TGA.

Differential scanning calorimetric. Heat flow properties of the dry and wet hydrogel materials were analyzed by differential scanning calorimetry (DSC) (Q2000, TA Instrument, New Castle, USA) as mentioned elsewhere.[3] Analysis was performed in nitrogen atmosphere, and the temperature range was kept between –35 and 90°C with a constant heating rate of 10°C/min. The surface water from both the hydrogel samples was completely removed by soaking with dry tissue paper before the DSC study.

Dynamic mechanical analysis. Thermomechanical properties were evaluated using dynamic mechanical analysis (DMA) (RSA-G2, TA Instruments, New Castle, USA), which measures the mechanical properties such as stiffness and damping of the produced hydrogel as described elsewhere.[17] Samples (size approximately: 8 mm diameter × 10 mm length) were subjected to analysis in compressive mode at a heating rate of 10°C min^{-1} in liquid nitrogen atmosphere. The temperature range applied was from –35 to 120°C at a constant frequency of 1 Hz.

Bone marrow stem cell isolation and culture

Rabbit bone marrow stem cells (BMSCs) were isolated aseptically from the tibia and femur of young adult (<12-week-old) white New Zealand rabbits (Species: *Oryctolagus cuniculus*). The isolation method was adopted from Poon et al.[18] with slight modifications and in accordance to Declaration of Helsinki in terms of ethical issues as the body part was obtained from slaughterhouse. Dulbecco's modified eagle medium (D8900, Sigma) supplemented with 10% fetal bovine serum (FB1001, Biosera) and 1% penicillin–streptomycin (P4333, Sigma) (culture medium) was used for in vitro cell culture. In brief, a fresh rabbit leg was obtained within hours of slaughter, and immersion in 70% alcohol for 15 min was needed for disinfection purpose prior to removal of hair, skin, and soft tissues attached to femur and tibia. Subsequently, the tibia and femur were excised from the joint, and metaphyseal ends of each bone were cut. Marrow from bone

was flushed out from midshaft with 10 ml of culture medium using a syringe through the opening at the ends. Then, the mushy thick liquid, which contained bone marrow, was collected in a 50-ml centrifuge tube and centrifuged at 2000 r/min for 5 min. The resulting cell pellet was re-suspended with 10 ml culture medium and plated in a T-75 culture flask and subsequently incubated in incubator under 5% CO_2 atmosphere, at 37°C and relative humidity of 95%. Medium was discarded together with unattached cells the next day, and only cells attached to bottom of culture flask remained in the flask. The culture flask was replenished with fresh culture medium, and the attached cells were allowed to propagate and grow to confluency for further use by changing medium every 2–3 days. Rabbit BMSCs at passage 3–6 were used in the cell study.

Cell cytotoxicity and proliferation evaluation

Determination of cell cytotoxicity and proliferation was based on evaluation of cell viability. Resazurin assay was adopted in this study as metabolic activity of viable cell reduces resazurin of blue color to pink-colored resorufin. Cytotoxicity of the fabricated hydrogel was determined by evaluating viability of fully confluent cell in direct contact with hydrogel. Briefly, 96-well molded hydrogels were soaked in distilled water to get rid of chemical residues after fabrication process (as described in 'Synthesis of hydrogels' section) prior to incubating the hydrogels with culture medium overnight in an incubator at 37°C with 5% CO_2 atmosphere. Meanwhile, 24-well plate with confluent BMSCs in each well was prepared by seeding 1×10^5 cell/ml for 3 days. Each well was assigned with one of the hydrogels and incubated in an incubator after BMSCs had grown to confluence in the wells. Wells with cells but without hydrogel were used as control. As for cell proliferation and attachment evaluation, proliferation of cell seeded directly on hydrogels was determined. Hydrogels were fabricated and placed in wells of a 24-well plate after rinsing with phosphate buffer solution (PBS). Subsequently, BMSCs at density of 1×10^4 cell in 20 µl aliquot were seeded on the hydrogel. Cells were given time to attach to the surface of hydrogel followed by topping up culture medium to the well to 1 ml after two hours. Resazurin assay was performed on hydrogels, which were moved to a new well plate after 1, 3, and 7 days incubation. Cells seeded directly on wells were used as control. Resazurin assay was carried out according to the instruction of the manufacturer. Briefly, resazurin working solution was prepared by adding 10% of resazurin stock solution (140 mg resazurin sodium salt powder (R7017, Sigma)) in 1 l PBS to culture medium. Five hundred microliters of resazurin working solution was added to each well and incubated in an incubator for four hours. Triplicates of 100 µl of reacted resazurin working solution from each well were transferred to respective wells in a fresh 96-well plate. Absorbances of reduced resazurin were measured at excitation wavelength of 570 nm and emission wavelength of 595 nm, using an FLUOstar Optima microplate reader (BMG Labtech, Offenburg, Germany). The viable cells were quantified as percentage of resazurin reduction using equation as described by the reagent manufacturer. The results were expressed as mean of reduction percentage ± standard deviation. Significance of the results obtained from control and hydrogel groups were statistically evaluated by paired *t*-test.

LIVE/DEAD® cell viability assays

Live/dead cell viability staining (L3224, Invitrogen) assays were performed according to the manufacturer's instructions on cells seeded within hydrogel to determine cell viability and attachment morphology of BMSCs in the hydrogel. The attachment and growth properties were visualized and captured by confocal microscopy with LIVE/DEAD® staining. Hydrogels were prepared by mixing UV sterilized 25:25:1 (w/w/w) of gel-like prepared biomaterial, PEGMA, and APS materials solutions to culture medium containing BMSCs at a density 1×10^6 cells/ml. TEMED solution was then added to the mixture (at 1:2 v/v ratio of TEMED:culture medium). The reaction mixture was quickly casted into the stainless steel mold and allowed to polymerize for 20 min at 25°C. After drying, the synthesized hydrogels were recovered from the casting molds and were transferred to a 100 mm petri dish containing 10 ml of culture medium. Hydrogels without cells prepared as described in the previous sections were considered as control. Both hydrogels with and without cells were incubated for 24 h. Hydrogels were prepared for LIVE/DEAD® staining and viewed under confocal microscope. According to the protocol provided by the manufacturer, hydrogels were prepared by removing the culture medium and rinsed with PBS. The LIVE/DEAD® reagent stock solutions were removed from the freezer and were allowed to warm to room temperature. One microliter of calcein (green dye) stock solution and 4 µl of EthD-1 (red dye) stock solution were mixed into 2 ml of PBS, and hydrogels were incubated with staining solution for 30–45 min at room temperature. After incubation, the excessive dye was removed, and the hydrogels were rinsed with PBS and the hydrogels were ready to be viewed under a confocal microscope.

Results and discussion

FTIR spectroscopy

From Figure 1, FTIR peaks of the hydrogel material were observed at 3292, 2935, 2869, 1638, 1555, 1468, 1162, and 1010 cm^{-1}. The peak signals at 1638 cm^{-1} represent –NHCONH–, 2935 and 2869 cm^{-1} represent $–CH_2$, and 1555 cm^{-1} represents amido group of PU.[19]

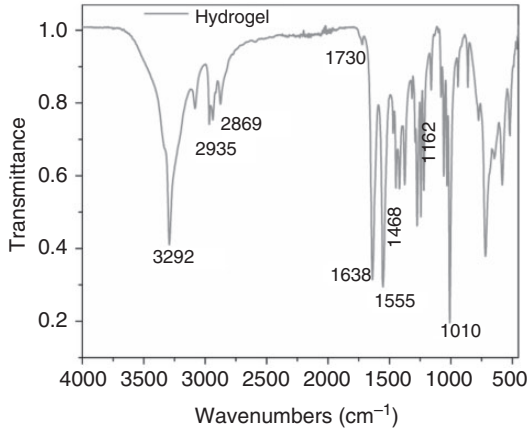

Figure 1. FTIR spectrum of the synthesized hydrogel material. FTIR: Fourier transform infrared.

The peak signals at 3290 cm^{-1} also represent N–H stretching, 1468 cm^{-1} represents aliphatic $–CH_2$ bending, 1162 and 1010 cm^{-1} represent symmetric stretching of C–O–C, and 1730 cm^{-1} is for the C=O group due to the influence of hydroxyl group from PHU.[20] Therefore, FTIR spectral analysis indicated that the synthesized hydrogel material is likely to be composed of PU and PHU.

NMR spectroscopy

In Figure 2, the ^{1}H NMR δ-shift peak signals were observed at 7.8 ppm, 3.01 ppm, 2.55 ppm, 2.50 ppm, 2.1 ppm, and 1.65 ppm. The peak signal at 7.8 ppm was attributed to RCONH of PU, 2.50 and 1.65 ppm from symmetric H in PU, 2.1 ppm attributed to protons from the two different *R* groups in PU, 3.01 ppm from NH_2 of PHU, and 2.55 ppm attributed to NH of PHU.[21,22]

In Figure 3, the δ-shift peak signals were observed at 172 ppm, 32.5 ppm, 32.6 ppm, 39–42 ppm, and 60.8 ppm. The peak signal at 172 ppm was attributed to the influence of C=O from PU, the peak signals at 32.5 and 32.6 ppm were attributed to the influence of NH and NH_2 group from PHU, the peak signals at 39–42 ppm (highest peak) were attributed to the rest of the carbons of the *R* and *R*′ of PU, and the peak signal at 60.8 ppm indicated the influence of the hydroxyl group of the

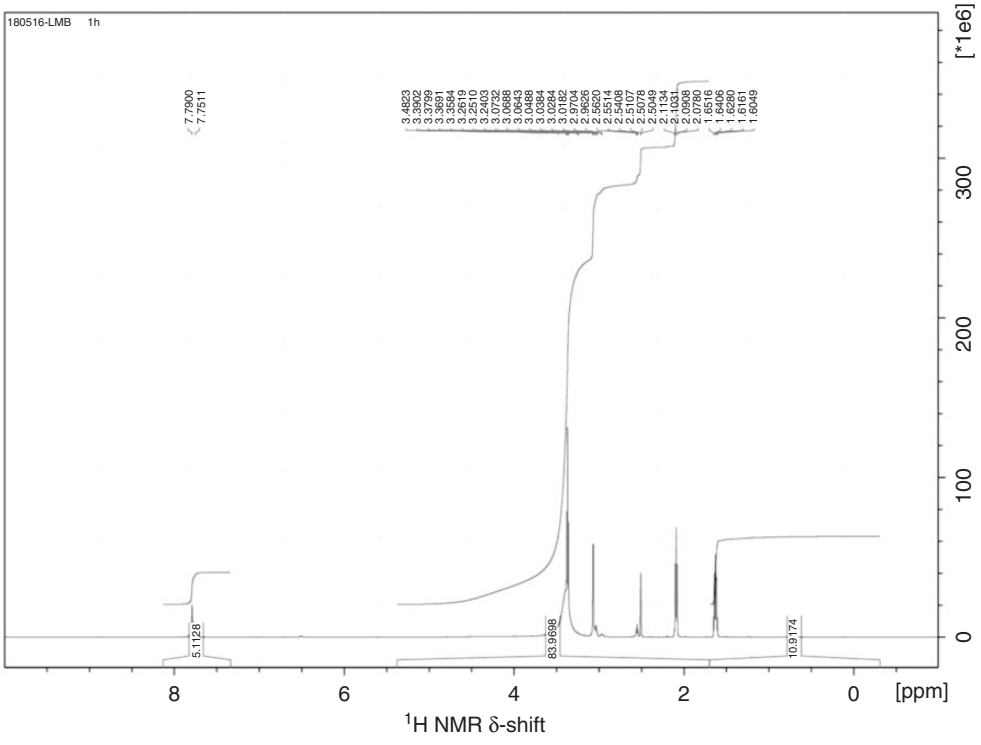

Figure 2. ^{1}H NMR spectrum of the synthesized hydrogel material with identified peaks. ^{1}H NMR: ^{1}H nuclear magnetic resonance.

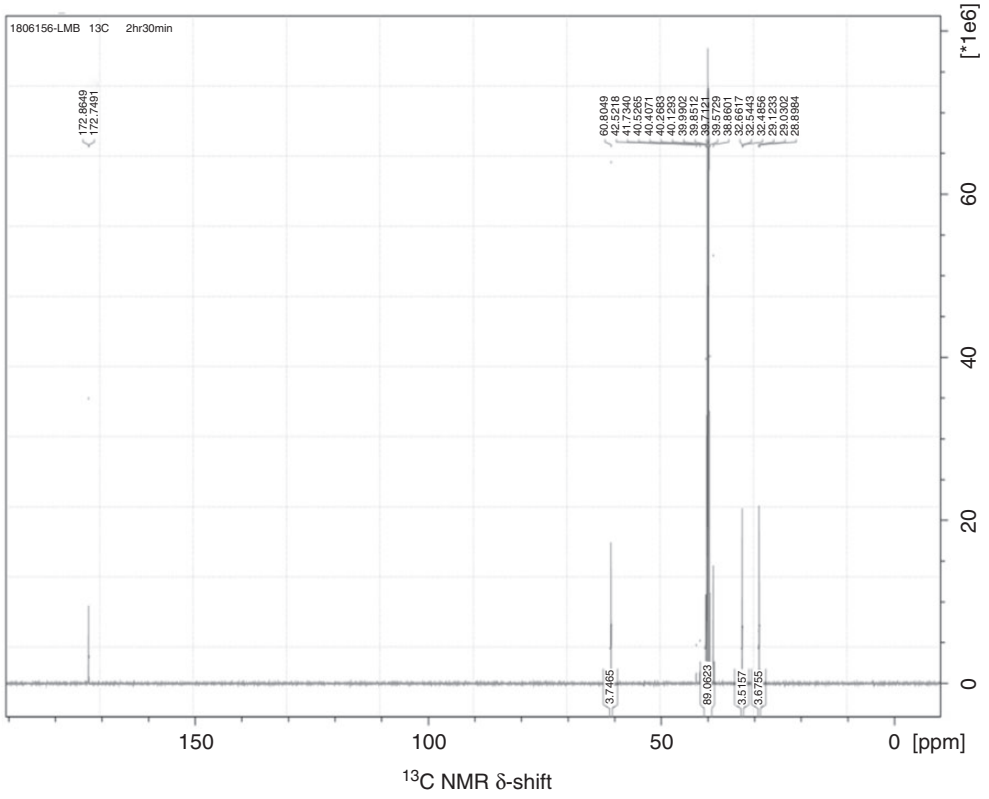

Figure 3. ^{13}C NMR spectrum of the synthesized hydrogel material with identified.
^{13}C NMR: ^{13}C nuclear magnetic resonance.

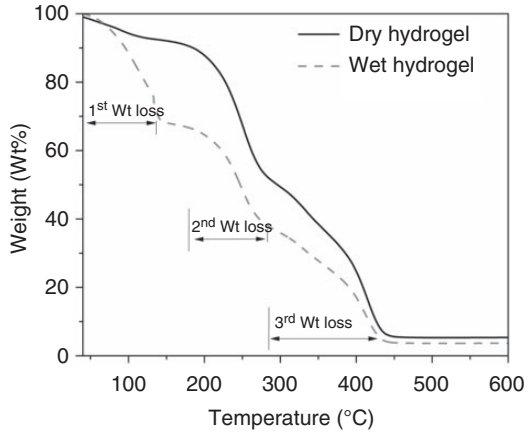

Figure 4. TGA plots of the dry and wet hydrogels indicate three major weight losses for both.
TGA: thermogravimetric analysis.

PHU.[21,22] Therefore, a probable structure of the hydrogel could be PU and PHU based block copolymer as shown in end product of Scheme 2.

Thermogravimetric analysis

Thermal degradation nature of both dry and wet hydrogels was found to be similar. Since wet hydrogel contained more water, its weight loss was noticeably faster than that of dry hydrogel. The first decrease in the weight percentage of the wet hydrogel material (around 32 wt %) was observed from around 40–150°C, where the steepest part was around 100°C (Figure 4) which indicated the evaporation of absorbed water in the hydrogel. The second weight loss (nearly 30 wt %) between 170 and 290°C and third weight loss (nearly 34 wt %) between 290 and 430°C clearly pointed to the thermal degradation of the organic fraction of the block copolymer from the two blocks. There was no further weight loss after 430°C. The second weight loss is attributed to the combustion of PHU in the hydrogel. The third weight loss around 400°C was attributed to the combustion of PU and PEGMA, which were used to prepare the hydrogel.

Differential scanning calorimetry

Two significant DSC peaks were found for both dry and wet hydrogels. From DSC thermogram (Figure 5), the first endothermic peak at around –12°C–7°C indicated mainly the melting of absorbed frozen water for the wet hydrogel as well as breaking of hydrogen bonds between the polymer chains. Another endothermic peak of the wet hydrogel at around 76°C pointed to the evaporation of water

molecules along with some organics. On the other hand, dry hydrogel showed two sharp endothermic peaks at around –2 and 0°C due to the breaking of hydrogen bonds between the polymer chains of the polymer and a small amount of adsorbed water, respectively. Since some organics present in the dry hydrogel had lower melting point (nearly 58°C) than water, the second endothermic peak of the dry hydrogel was found to be lower than wet hydrogel.

Dynamic mechanical analysis

The dynamic mechanical properties of the hydrogel were characterized by the change in loss modulus (E'', MPa), storage modulus (E', MPa), and energy dissipation factor (tan $\delta = E''/E'$) as a function of temperature. The maximum storage modulus of the hydrogel was found at temperature around 0°C (see Figure 6). Maximum loss of storage modulus was observed in the range of 0–20°C. Since the rate of change in loss energy of this material is very high compared to the rate of change in storage energy, tan δ becomes more than 0.5 (tan δ peak around 37°C in Figure 6). Therefore, this newly developed hydrogel can be used to control the mechanical and degradation properties of tissue expander hydrogels.[23,24]

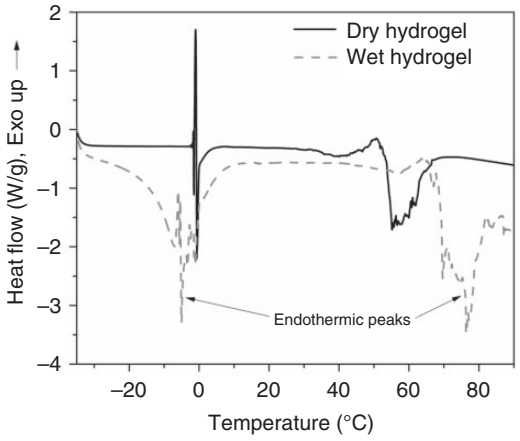

Figure 5. Differential scanning calorimetric plots of the dry and wet hydrogels indicate two major endothermic peaks for both.

Cytotoxicity and proliferation evaluation

A rabbit's BMSCs were used as a cellular model during evaluation of the hydrogel's cytotoxicity following resazurin assay (see Figure 7). Percentage of reduction is directly proportional to the number of viable cell. The results obtained from cytotoxic evaluation indicated a noticeable increase in cell proliferation with 24–72 h incubation for both sample and control. The cell in the wells had been confluent when the hydrogel was first introduced to the well. Slight increase in cell number shown by this study was due to the layer formation of neocells over the other cell layers, which was confirmed by inverted microscopy observation (see Figure 8). The observation made was also supported by other studies.[2,3] With reference to the control sample, the percentage of reduction by cell incubated with sample had similar cell proliferation rate. The results in Figures 7 and 8 with high concentrated stem cells indicated that there was no cytotoxic effect because

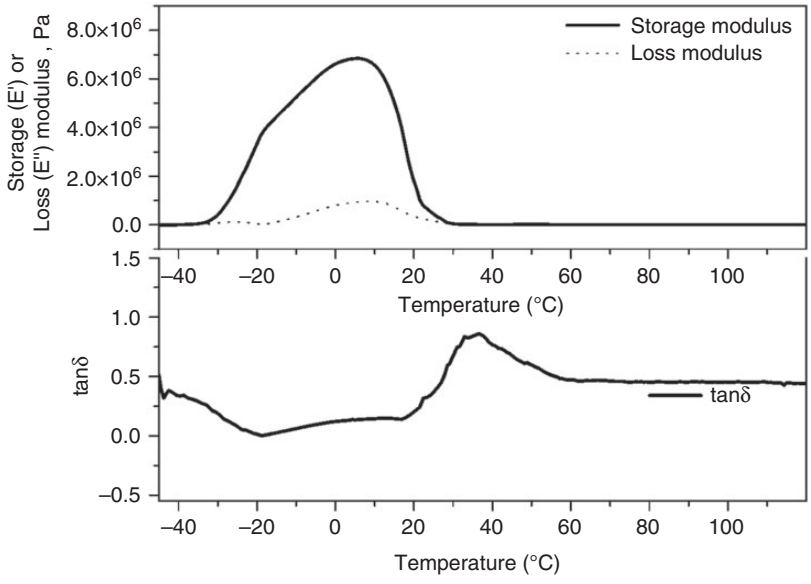

Figure 6. Dynamic mechanical analysis plots of the hydrogel (above – storage (thick farm line) and loss modulus (dotted line); bottom – tan δ peak or damping factor (thin farm line)).

of the negligible difference between hydrogel samples and control i.e. hydrogels did not cause detectable death of cell. There was no significant difference ($p > 0.05$) between the control and hydrogel samples after incubation from 48 to 72 h. Thus, it can be concluded that the synthesized hydrogel showed negligible cytotoxic effects and is bio-inert toward healthy BMSCs of rabbits.

According to the results obtained from the resazurin assay on rabbit BMSCs seeded directly on hydrogel (Figure 9), a significant difference between proliferation of cell seeded directly on hydrogel samples and well (i.e. controls) was observed throughout the incubation period from day 1 to day 7. Cell number increasing in the well without hydrogel was most significant

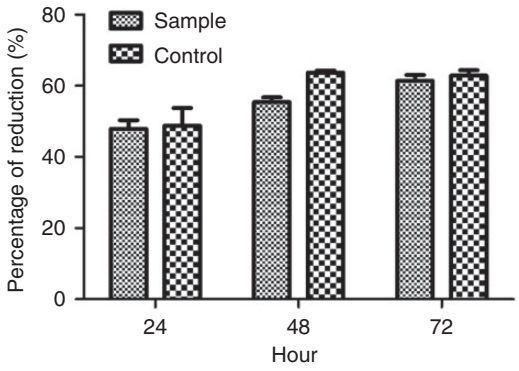

Figure 7. Percentage of reduction in resazurin assay which indicates viability of rabbit BMSCs incubated with hydrogel in well for 24, 48, and 72 h. Sample represents cell incubated with hydrogel and control represents cell without incubation with hydrogel, with $n = 6$. Note: There was no significant difference between the hydrogel and control after incubation ($p > 0.05$).
BMSCs: bone marrow stem cells.

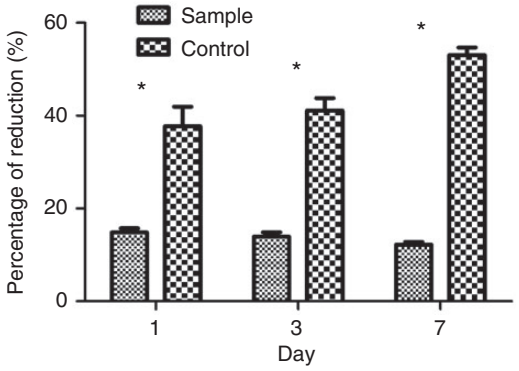

Figure 9. Percentage of reduction in resazurin assay which indicates viability of rabbit BMSCs seeded directly on hydrogel for 1, 3, and 7 days. Sample represents cell seeded on hydrogel and control represents cell on well and without hydrogel, with $n = 6$, where * represents significant low percentage of reduction of sample compared to control at $p < 0.05$. Note: The percentage reduction was stationary for the stem cell seeded hydrogel samples from day 1 to day 3.
BMSCs: bone marrow stem cells.

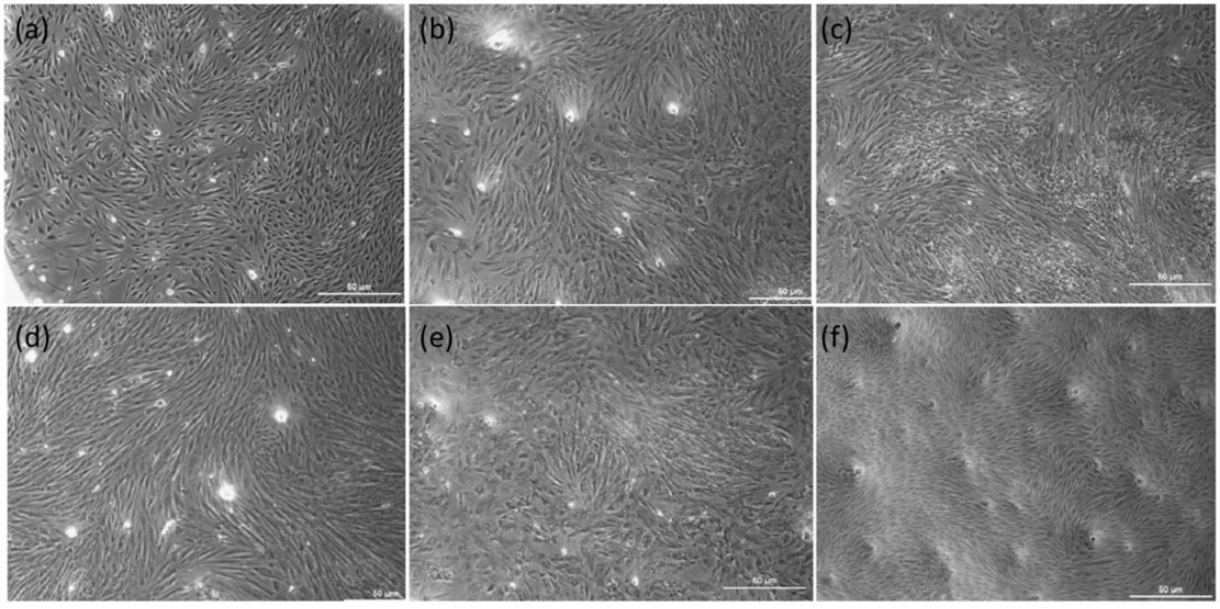

Figure 8. Rabbit BMSCs under inverted microscopic view of (a–c) cells in direct contact with the hydrogel and (d–f) control for (a, d) 24, (b, e) 48, and (c, f) 72 h. Bar scale for all images is 50 μm.
BMSCs: bone marrow stem cells.

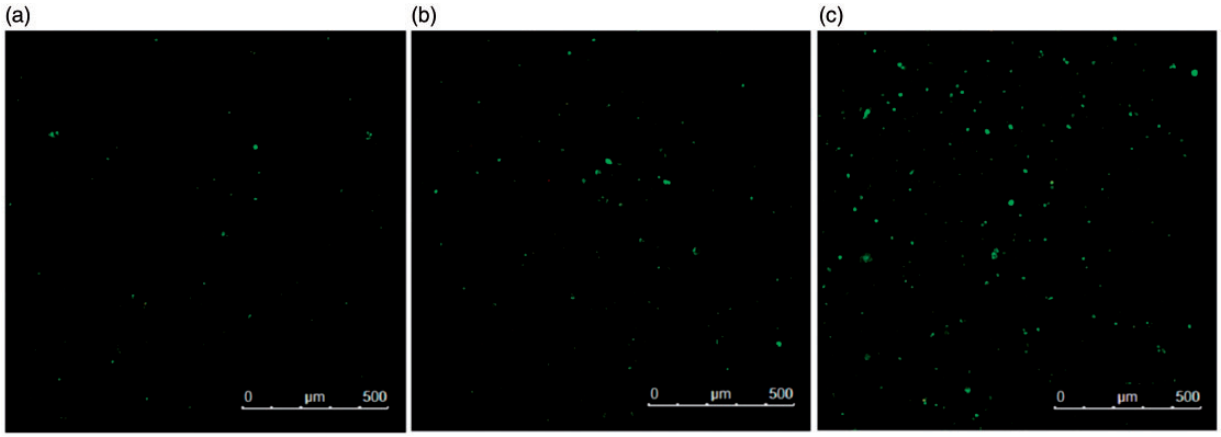

Figure 10. Fluorescence microscopic images of live/dead staining of cell encapsulated and incubated within hydrogels using confocal microscope are shown. Images show (a) hydrogel without cells and with stain, (b) hydrogel with cells and without stain, and (c) hydrogel with cells and with stain. (Color image is available only for soft copy in online and not for printed copy).

from day 3 to day 7. On the other hand, increase in cell proliferation for those seeded directly on hydrogel samples from day 1 to day 7 was poor compared to the controls. The low percentage of reduction in cell seeded directly on hydrogel could be due to the smooth surface of hydrogel. It is a clear indication of bio-inertness of the hydrogel. Hence, the present bio-inert hydrogel may help to improve the immunocompatibility of the tissue expanders.[25]

For this study, a direct contact test is an alternative solution to assess the cytotoxicity of the hydrogel. The test can be improved by using a hydrogel with different volume or weight as variables. Briefly, cytotoxicity level of the hydrogel was determined by the difference in the volume of hydrogel and the desired volume ratio of the hydrogel to the culture medium. By using different volumes of the hydrogels, it could be possible to measure the lethal dose. One problem with this technique could be that a larger volume of hydrogel might be too heavy for the cell to handle. The cells might die due to permanent compression of the heavy hydrogels rather than due to leaching by-products. The BMSCs response in terms of cell attachments and proliferation was shown by a similar technique of Gumel et al.[15] The main reason that contributes to the significant differences seen between cells seeded on hydrogel and control is due to surface quality. The smoothness and sliminess surface of the hydrogel might not be conducive for cell attachment. For example, agarose which is a natural polysaccharide polymer material, generally extracted from seaweed, is widely synthesized as hydrogel for applications in tissue engineering scaffold or coating material and does not allow cell attachment on the surface. Cell attachment to the agarose surface is promoted by the addition of cell adhesion moieties.[26] For example, the agarose hydrogel can be coupled with an extracellular matrix protein such as laminin to improve cell attachment.[27] One of the ways that might improve the cell attachments to the surface of the hydrogels is by coating it with extracellular matrix proteins such as collagen, fibronectin, and laminin.[28] Therefore, the present investigation might solve the fibrosis problems by controlling the formation of excess fibrous connective tissues in an organ at a reactive state.[29]

LIVE/DEAD® cell viability assays and confocal microscope

Results of cytotoxicity and proliferation assays indicate quantitative information of cell growth but the qualitative cytotoxicity results of the hydrogel can be evaluated from confocal microscopy observation.[30] Interestingly, when the neat hydrogel samples were viewed under the confocal microscope and without staining, tiny spots of green colors were clearly visible (micrograph not shown). The green and red colors were also observed in the stained sample without cells (Figure 10(a)). This clearly indicated that the synthesized hydrogel exhibited (self) fluorescent properties.

The confocal microscopic images under fluorescence excitation using LIVE/DEAD® staining on the cell encapsulated in hydrogel showed significant difference compared to the others. Abundant tiny green spots indicated the viability of stem cells encapsulated by hydrogels after 7 days incubation. The large cells present in the hydrogel were not visible entirely because the self-fluorescence of the hydrogel itself hindered the detection of specific fluorescent signals or stains, particularly when the wanted signals were relatively dimmer as suggested by other studies.[31] Therefore, the hydrogel has self-fluorescence effect besides it being a conducive milieu for cell proliferation. The newly discovered self-fluorescence property of the

synthesized hydrogel material made it a potentially useful contrast agent in other applications, such as magnetic resonance imaging.

Conclusions

The structural, mechanical, and biocompatibility studies of a novel hydrogel material are reported. The starting compound comprised PU and PHU as primary building blocks and synthesized via lipase catalysis. It was used alongside polyethylene glycol, APS, and tetramethylethylenediamine to produce a hydrogel via radical polymerization. Biocompatibility tests showed the hydrogel as an inert material to the rabbit bone stem cells. Apart from its bio-inertness, the hydrogel exhibited self-fluorescence properties under specific excitation wavelength and might potentially be used as a contrast agent in imaging applications. Therefore, the present bio-inert hydrogels can potentially be adopted in medicine as well as in excellent tissue expander, which is used in wound healing, dental, plastic, and in advanced surgeries.[23–25,29]

Declaration of conflicting interests

The author(s) declared no potential conflicts of interest with respect to the research, authorship, and/or publication of this article.

Funding

The author(s) disclosed receipt of the following financial support for the research, authorship, and/ or publication of this article: The study was partially funded by University of Malaya Postgraduate Research Grant (PPP) No. PG038-2015B.

ORCID iD

Sumit Pramanik http://orcid.org/0000-0003-0455-1582

References

1. Ansari NF, Annuar MSM and Pingguan-Murphy B. A porous medium-chain-length poly (3-hydroxyalkanoates)/hydroxyapatite composite as scaffold for bone tissue engineering. *Eng Life Sci* 2017; 17: 420–429.
2. Pramanik S, Ataollahi F, Pingguan-Murphy B, et al. In vitro study of surface modified poly (ethylene glycol)-impregnated sintered bovine bone scaffolds on human fibroblast cells. *Sci Rep* 2015; 5: 9806 (pp.1–11).
3. Pramanik S and Kar KK. Functionalized poly (ether ether ketone): improved mechanical property and acellular bioactivity. *J Appl Polym Sci* 2012; 123: 1100–1111.
4. Smith J, Radzi Z and Czernuszka J. The effects of hot pressing on the swelling behavior of P (MMA-*co*-NVP) hydrogel discs. *Polym Eng Sci* 2015; 55: 1290–1295.
5. Modjarrad K and Ebnesajjad S. *Handbook of polymer applications in medicine and medical devices*. New York: Elsevier, 2013.
6. Lee KY and Mooney DJ. Hydrogels for tissue engineering. *Chem Rev* 2001; 101: 1869–1880.
7. Pan J-F, Yuan H-F, Guo C-A, et al. One-step cross-linked injectable hydrogels with tunable properties for space-filling scaffolds in tissue engineering. *RSC Adv* 2015; 5: 40820–40830.
8. Drury JL and Mooney DJ. Hydrogels for tissue engineering: scaffold design variables and applications. *Biomaterials* 2003; 24: 4337–4351.
9. Mellati A, Dai S, Bi J, et al. A biodegradable thermosensitive hydrogel with tuneable properties for mimicking three-dimensional microenvironments of stem cells. *RSC Adv* 2014; 4: 63951–63961.
10. Discher DE, Janmey P and Wang YL. Tissue cells feel and respond to the stiffness of their substrate. *Science* 2005; 310: 1139–1143.
11. Yetisen AK, Naydenova I, da Cruz Vasconcellos F, et al. Holographic sensors: three-dimensional analyte-sensitive nanostructures and their applications. *Chem Rev* 2014; 114: 10654–10696.
12. Kunisaki SM and Fauza DO. Chapter 80: current state of clinical application A2 – Lanza, Robert. In: R Langer and J Vacanti (eds) *Principles of tissue engineering*. 4th ed. Boston: Academic Press, 2014, pp.1687–1696.
13. Uyama H, Takeya K and Kobayashi S. Enzymatic ring-opening polymerization of lactones to polyesters by lipase catalyst: unusually high reactivity of macrolides. *BCSJ* 1995; 68: 56–61.
14. Uyama H, Namekawa S and Kobayash S. Mechanistic studies on the lipase-catalyzed ring-opening polymerization of lactones. *Polym J* 1997; 29: 299–301.
15. Gumel AM, Razaif-Mazinah MRM, Anis SNS, et al. Poly (3-hydroxyalkanoates)-*co*-(6-hydroxyhexanoate) hydrogel promotes angiogenesis and collagen deposition during cutaneous wound healing in rats. *Biomed Mater* 2015; 10: 045001 (pp.1–14).
16. Manna A, Pramanik S, Tripathy A, et al. Design and development of an in situ synthesized layered double hydroxide structure of Fe-induced hydroxyapatite for drug carriers. *RSC Adv* 2016; 6: 25549–25561.
17. Tripathy A, Pramanik S, Manna A, et al. Synthesis and characterizations of novel Ca-Mg-Ti-Fe-oxides based ceramic nanocrystals and flexible film of polydimethylsiloxane composite with improved mechanical and dielectric properties for sensors. *Sensors* 2016; 16: 292 (pp.1–22).
18. Poon CT, Abas W, Kim K, et al. (eds) Effect of herbal extracts on rat bone marrow stromal cells (BMSCs) derived osteoblast – preliminary result. In: *5th Kuala Lumpur international conference on biomedical engineering*, Kuala Lumpur, Malaysia, 2011. New York: Springer.
19. Gao C, Jin YZ, Kong H, et al. Polyurea-functionalized multiwalled carbon nanotubes: synthesis, morphology, and Raman spectroscopy. *J Phys Chem B* 2005; 109: 11925–11932.

20. McCarthy SJ, Meijs GF, Mitchell N, et al. In-vivo degradation of polyurethanes: transmission-FTIR microscopic characterization of polyurethanes sectioned by cryomicrotomy. *Biomaterials* 1997; 18: 1387–1409.
21. Zhang F, Jiang X, Zhu X, et al. Preparation of uniform and porous polyurea microspheres of large size through interfacial polymerization of toluene diisocyanate in water solution of ethylene diamine. *Chem Eng J* 2016; 303: 48–55.
22. Cornille A, Serres J, Michaud G, et al. Syntheses of epoxyurethane polymers from isocyanate free oligo-polyhydroxyurethane. *Eur Polym J* 2016; 75: 175–189.
23. Garner J, Davidson D, Eckert GJ, et al. Reshapable polymeric hydrogel for controlled soft-tissue expansion: in vitro and in vivo evaluation. *J Control Release* 2017; 262: 201–211.
24. Agrawal K and Agrawal S. Tissue regeneration during tissue expansion and choosing an expander. *Indian J Plast Surg* 2012; 45: 7–15.
25. Hong JK and Kwon SM. Application of tissue engineering in stem cell therapy. *JBiSE* 2014; 7: 67–74.
26. Lewitus DY, Landers J, Branch JR, et al. Biohybrid carbon nanotube/agarose fibers for neural tissue engineering. *Adv Funct Mater* 2011; 21: 2624–2632.
27. Yu X, Dillon GP and Bellamkonda RV. A laminin and nerve growth factor-laden three-dimensional scaffold for enhanced neurite extension. *Tissue Eng* 1999; 5: 291–304.
28. Hudson AE, Carmean N and Bassuk JA. Extracellular matrix protein coatings for facilitation of urothelial cell attachment. *Tissue Eng* 2007; 13: 2219–2225.
29. Vegas AJ, Veiseh O, Doloff JC, et al. Combinatorial hydrogel library enables identification of materials that mitigate the foreign body response in primates. *Nat Biotechnol* 2016; 34: 345–352.
30. Xian W. *A laboratory course in biomaterials*. Boca Raton, FL: CRC Press, 2009.
31. Neumann M and Gabel D. Simple method for reduction of autofluorescence in fluorescence microscopy. *J Histochem Cytochem* 2002; 50: 437–439.